

Markus Rottmann*, Jannik Zürn, Ufuk Arslan, Karin Klingel and Olaf Dössel

Effects of fibrosis on the extracellular potential based on 3D reconstructions from histological sections of heart tissue

A proof of concept simulation study

DOI 10.1515/cdbme-2016-0147

Abstract: Atrial fibrillation is the most common arrhythmia. However, the mechanisms of AF are not completely understood. It is known that fractionated signals are measured in AF but the etiology of fractionated signals is still not clear. The central question is to evaluate the effects of segmented fibrotic areas in histological tissue sections on the extracellular potential in a simulation study. We calculated the transmembrane voltages and extracellular potentials from the excitation wave front around a 3D fibrotic area from mouse hearts that were reconstructed from histological tissue sections. Extracellular potentials resulted in fragmented signals and differed strongly by stimulations from different directions. The transmural angle of the excitation waves had a significantly influence on the signal morphologies. We suggest for future clinical systems to implement the possibility for substrate mapping by stimulations from different directions in sinus rhythm.

Keywords: atrial fibrillation; experiment; extracellular potential; fibrosis; finite element simulation; histological tissue sections; mouse model of myocarditis.

1 Introduction

AF is a common arrhythmia and frequently fractionated signals are measured [1, 2]. The mechanisms of AF and

the correlation with typically unipolar signals and in particular fractionated signals are not well understood [3–5]. There are simulation studies of correlations of intracardiac signals in AF [6, 7] and correlations with fibrosis, but the fibrotic patterns were in the whole myocardium between endocardium and epicardium and the implementation was based on random numbers [8] or implemented in a 2D area [9]. For the first time we calculated extracellular potentials from the excitation around a 3D fibrotic area reconstructed from real fibrotic areas obtained in histological heart tissue sections. In this proof of concept the correlation between fibrotic area and fractionated signals is presented. Also, the influences of the transmural angle of the wave front and stimulations from different directions on the extracellular potential are presented.

2 Methods

2.1 Histological tissue sections

In order to investigate cardiac fibrosis *in vivo*, we used a mouse model of chronic CVB3 myocarditis. Hearts were obtained 4 weeks after CVB3 infection of ABY/SnJ mice, at a time point when fibrosis is obvious. The hearts were fixed in 4% paraformaldehyde and embedded in paraffin. 5 μm thick tissue sections covering the right and left ventricle were cut with a distance of 10 μm and stained with Sirius red. The red staining illustrates myocardial fibrosis. Images from the same area of 60 consecutive tissue sections were taken with a Zeiss Axioskop 40 microscope and used for reconstruction by manual registering. Figure 1 shows exemplarily histological tissue sections of the right and left ventricle of 10x and 100x magnification.

*Corresponding author: Markus Rottmann, KIT- Institute of Biomedical Engineering, Karlsruhe Institute of Technology, Karlsruhe, Germany, E-mail: Markus.Rottmann@kit.edu

Jannik Zürn, Ufuk Arslan and Olaf Dössel: KIT - Institute of Biomedical Engineering, Karlsruhe Institute of Technology, Karlsruhe, Germany

Karin Klingel: Department of Molecular Pathology, University Hospital Tübingen, Germany

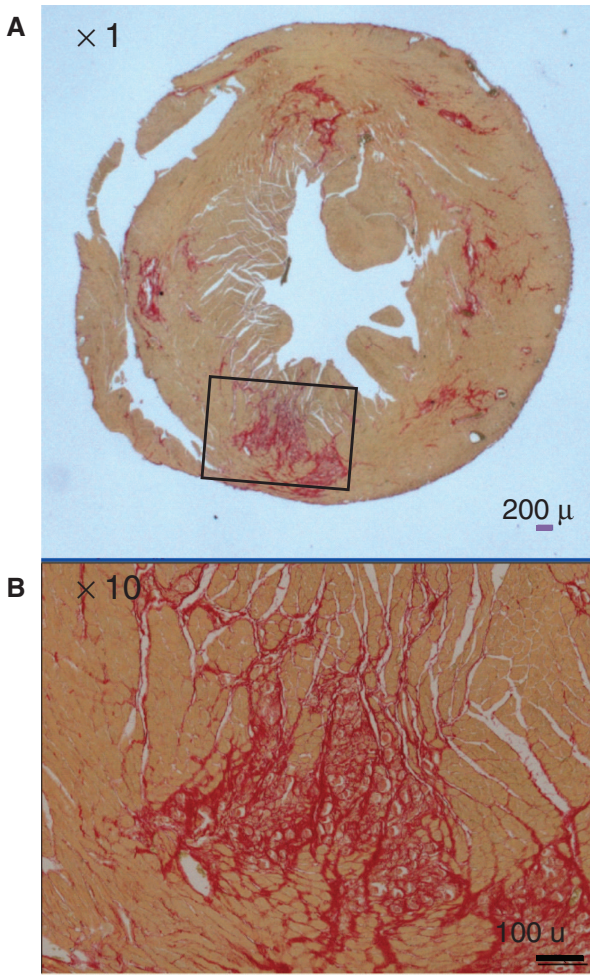


Figure 1: High resolution image of ventricular histological tissue sections at a microscopic magnification of $\times 10$ (A). (B) is the inset of (A) at a magnification of $\times 100$. The Sirius red staining illustrates myocardial fibrosis.

2.2 3D reconstructions from histological tissue sections

The dimensions of the histological images were $750 \mu\text{m}$ by $1000 \mu\text{m}$. In order to obtain a 3D reconstruction of the fibrotic tissue by using identified landmarks, we manually segmented fibrosis of each image obtained from the same area of consecutive heart tissue sections. We created binary images in which the pixels corresponding to fibrotic tissue are marked with 1, and the other tissue types with 0. Then we rescaled the images in order to get cubic voxels with edge length of $12.5 \mu\text{m}$. Then we applied a scaling factor of 20 to get from mouse-size atrium to human-size atrium.

In a further step we created a 3D model of the fibrotic tissue by stacking the single segmented images on top of each other, see Figure 2. The 3D reconstruction of

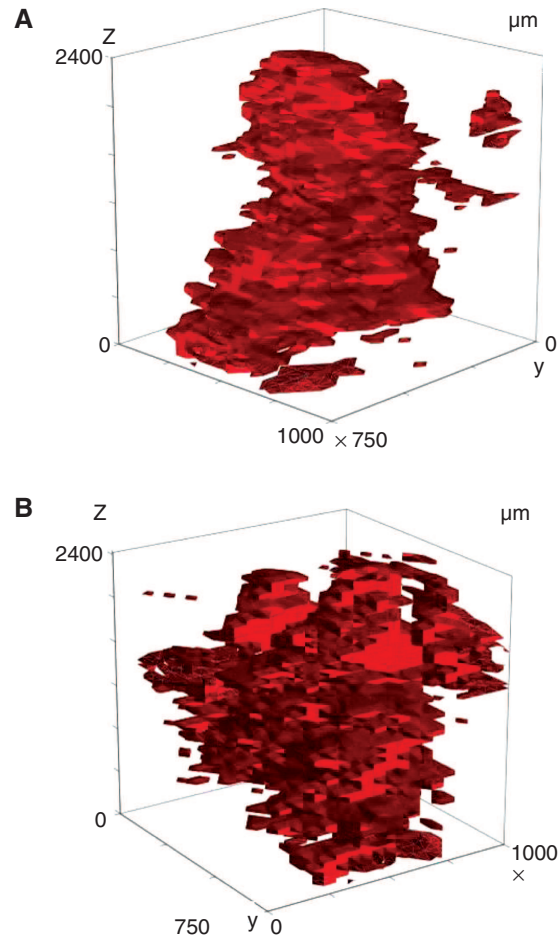


Figure 2: 3D Reconstruction of the fibrotic tissue from segmented histological tissue sections in (A) front view, (B) behind view.

the fibrotic area consisted of voxels with edge length of 0.25 mm .

2.3 Calculation of cardiac potentials and modelling of fibrosis

Transmembrane voltages were calculated using the monodomain equation with the parallel solver aCELLerate [10].

$$r \cdot \sigma_M r V_M = \beta \left(C_m \frac{dV_m}{dt} I_{mem} \right) = \beta I_m \quad (1)$$

V_M , represents the transmembrane voltage, σ_M the bulk conductivity and β the cell- surface to volume ratio [8]. By forward calculation [8] extracellular potentials were calculated based on transmembrane source current density [9] with a sampling rate of 1 kHz. To describe ventricular behaviour the cell model of Ten Tusscher et al. was used. The simulation geometry consisted on a regular grid of cubic elements. The 3D patch had the size of

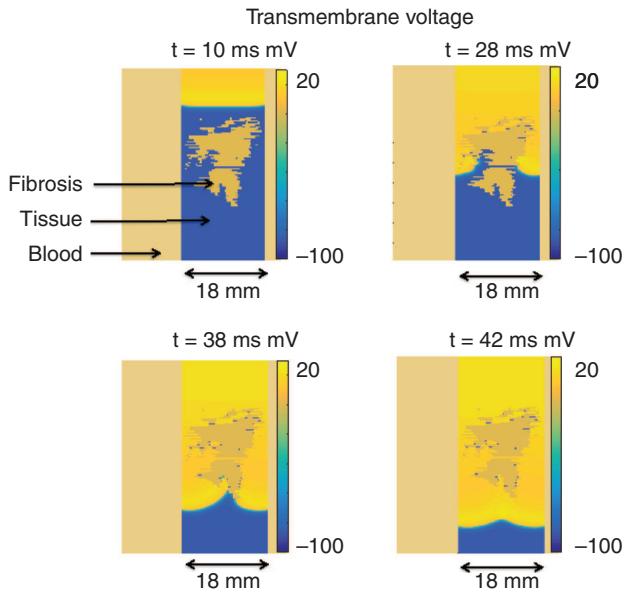


Figure 3: Transmembrane voltages of an excitation around fibrotic area at the times 10 ms, 28 ms, 38 ms and 42 ms.

$200 \times 200 \times 200$ voxels with the voxel length 0.25 mm. The manually segmented fibrotic area was implemented in healthy tissue. Segmented collagenous structures from the histological tissue sections were modelled as fibrotic elements without consideration of tissue conductivity and sodium handling [8].

3 Results

3.1 Transmembrane voltages of plane wave stimulation

The tissue was stimulated in the upper part of the tissue. In Figure 3 the meandering of the excitation wave fronts around the fibrotic area is depicted at different times. The transmural angle and the conduction velocity of the splitted excitation fronts varied at different times. Because of the reaction diffusion behaviour the excitation became a nearly plane wave again in the lower part.

3.2 Transmembrane voltages and extracellular potentials of stimulation with transmural angle

Transmembrane and extracellular potentials of the stimulation in the left upper corner ($10 \times 10 \times 10$ voxels) resulted in fractionated extracellular signals, see Figure 4.

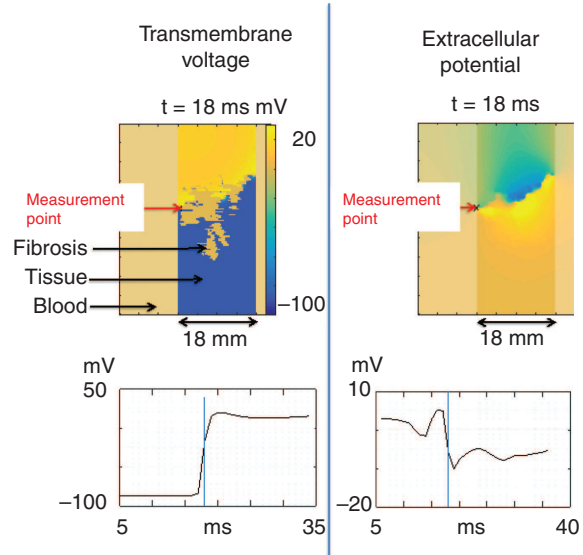


Figure 4: Left: Excitation wave front of the transmembrane voltage at time 18 ms and corresponding signal at the measurement point. Right: Excitation wave front of the extracellular potential at time 18 ms and corresponding signal.

3.3 Signal analysis

Figure 4 shows the resulting transmembrane potential at the selected measurement point in the first tissue layer close to the blood layers. Furthermore the corresponding extracellular potential at the first blood layer close to the tissue is presented. The measured unipolar signal was strongly deformed from ideal signal form of healthy tissue. Unipolar signals measured at the endocardium were on the one hand dependent on the fibrosis and on the other hand dependent on the direction of the wave front. Especially the transmural angle of the wave front had a significant influence on the signal form.

4 Discussion and summary

This work presents the first simulation study of 3D fibrosis reconstructed from histologically reconstructed murine heart tissue. We present a proof of principle that fractionated signals can be measured from real fibrotic areas reconstructed from histological tissue sections. The patterns of fibrosis are similar to those observed in humans. On the one hand fractionated signal morphologies from unipolar recordings could be correlated with fibrotic areas, on the other hand the signal morphologies were strongly dependent on the parameters of the excitation wave direction

and transmural angle. Future clinical systems might implement fibrosis mapping by stimulations from various directions in sinus rhythm. We used several simplifications in this proof of concept simulation study in the 3D reconstruction of fibrosis. Furthermore we translated animal heart fibrosis to a human model of fibrosis.

Author's Statement

Research funding: The author state no funding involved. Conflict of interest: Authors state no conflict of interest. Material and methods: Informed consent: Informed consent is not applicable. Ethical approval: The research related to animal use complies with all the relevant national regulations and institutional policies for the care and use of animals.

References

- [1] Nademanee K, McKenzie J, Kosar E, Schwab M, Sunsaneewitayakul B, Vasavakul T, et al. A new approach for catheter ablation of atrial fibrillation: mapping of the electrophysiologic substrate. *J Am Coll Cardiol*. 2004;43:2044–53.
- [2] de Jong S, van Veen TA, van Rijen HV, de Bakker JM. Fibrosis and cardiac arrhythmias. *J Cardiovasc Pharm*. 2011;57:630–8.
- [3] Spach MS, Heidlage JF, Dolber PC, Barr RC. Mechanism of origin of conduction disturbances in aging human atrial bundles: experimental and model study. *Heart Rhythm*. 2007;4:175–85.
- [4] Jacquemet V, Henriquez CS. Genesis of complex fractionated atrial electrograms in zones of slow conduction: a computer model of microfibrosis. *Heart Rhythm*. 2009;6:803–10.
- [5] Jacquemet V, Henriquez CS. Genesis of complex fractionated atrial electrograms in zones of slow conduction: a computer model of microfibrosis. *Heart Rhythm*. 2009;6:803–10.
- [6] Rottmann M, Keller MW, Oesterlein T, Seemann G, Doessel O. Comparison of different methods and catheter designs to estimate the rotor tip position - a simulation study. *Computing in Cardiology Conference*. 2014:133–136.
- [7] Rottmann M, Unger L, Kaltenbacher W, Seemann G, Loewe A, Krueger MW, et al. Methods for analyzing signal characteristics of stable and unstable rotors in a realistic heart model. *Computing in Cardiology Conference 2015*: 485–488.
- [8] Keller MW, Luik A, Soltan Abady M, Seemann G, Schmitt C, Dössel O, et al. Influence of three-dimensional fibrotic patterns on simulated intracardiac electrogram morphology. *Computing in Cardiology*. 2013.
- [9] Campos F, Wiener T, Prassl A, Weber Dos Santos R, Sanchez-Quintana D, Ahammer H, et al. Electro-anatomical characterization of atrial microfibrosis in a histologically detailed computer model. *IEEE Trans Biomed Eng*. 2013.
- [10] Seemann G, Sachse FB, Karl M, Weiss DL, Heuveline V, Doessel O. Framework for modular, flexible and efficient solving the cardiac bidomain equation using PETSC. *Mathematics in Industry*. 2010;15:363–9.